Distributed Control of Multi-Functional Grid-Tied Inverters for Power Quality Improvement

Jianbo Chen, *Graduate Student Member, IEEE*, Dong Yue, *Fellow, IEEE*, Chunxia Dou, *Member, IEEE*, Ye Li, Gerhard P. Hancke, *Life Fellow, IEEE*, Shengxuan Weng, Josep M. Guerrero, *Fellow, IEEE*, and Xiaohua Ding

***Abstract*— Multi-functional grid-tied inverters (MFGTIs) have been investigated recently for improving the power quality (PQ) of microgrids (MGs) by exploiting the residual capacity (RC) of distributed generators. Several centralized and decentralized methods have been proposed to coordinate the MFGTIs. However, with the increasing number of the MFGTIs, it demands a method with improved reliability and flexibility, which are characteristics of distributed framework that has not been introduced into the PQ improvement (PQI) field before. In this paper, we propose a distributed consensus method to undertake the PQI task. The task is proportionally shared among the MFGTIs according to their instant RCs. Besides, most of the existing methods assume that the RCs of the MFGTIs are sufficient for tackling the PQ problem (PQP), which is not always true. In the case of insufficient RC, the active power output of each MFGTI is scaled down by the same factor determined by a proposed leader-follower protocol to make room for the task. In summary, the PQP is dealt with in both cases of sufficient and insufficient RC under the distributed control framework. Finally, simulations and hardware-in-the-loop experiments of an MG consisting of three 10kVA MFGTIs are presented to verify the effectiveness of the proposed methods.**

***Index Terms*— Consensus method, distributed control, microgrid, multi-functional grid-tied inverter, power quality.**

Manuscript received May 22, 2020; revised November 4, 2020; accepted November 17, 2020. Date of publication December 17, 2020; date of current version January 12, 2021. This work was supported in part by the Leading-Edge Technology Program of Jiangsu Natural Science Foundation under Grant BK20202011, in part by the National Natural Science Foundation of China under Grant 61833008 and Grant 61933005, in part by the Science and Technology Project of NARI Technology Company Ltd., on "Research on Key Technologies for Simulation and Evaluation of Comprehensive Energy Systems" under Grant 2019out129, and in part by the VILLUM FONDEN under the VILLUM Investigator: Center for Research on Microgrids (CROM) under Grant 25920. This article was recommended by Associate Editor T. Fernando. *(Corresponding authors: Dong Yue; Chunxia Dou; Gerhard P. Hancke).*

Jianbo Chen and Dong Yue are with the College of Automation, Nanjing University of Posts and Telecommunications, Nanjing 210023, China, and also with the College of Artificial Intelligence, Nanjing University of Posts and Telecommunications, Nanjing 210023, China (e-mail: jianbo686@aliyun.com; medongy@vip.163.com).

Chunxia Dou and Shengxuan Weng are with the Institute of Advanced Technology, Nanjing University of Posts and Telecommunications, Nanjing 210023, China (e-mail: cxdou@ysu.edu.cn; shxweng@gmail.com).

Ye Li is with Shanghai KeLiang Technology and Engineering Company Ltd., Shanghai 200233, China (e-mail: ye.li@keliangtek.com).

Gerhard P. Hancke is with the College of Automation, Nanjing University of Posts and Telecommunications, Nanjing 210023, China, and also with the Department of Electrical, Electronic and Computer Engineering, University of Pretoria, Pretoria 0002, South Africa (e-mail: g.hancke@ieee.org).

Josep M. Guerrero is with the Center for Research on Microgrids (CROM), Department of Energy Technology, Aalborg University, 9220 Aalborg East, Denmark (e-mail: joz@et.aau.dk).

Xiaohua Ding is with NARI Technology Company Ltd., Nanjing 211000, China (e-mail: dingxiaohua@sgepri.sgcc.com.cn).

Color versions of one or more figures in this article are available at https://doi.org/10.1109/TCSI.2020.3040253.

Digital Object Identifier 10.1109/TCSI.2020.3040253

I. Introduction

With the increasing concerns on environmental issues and the energy crisis, distributed generators (DGs), such as photovoltaic (PV) and wind-turbine (WT), have widely been adopted and connected to the utility grid (UG) as a supplement to the traditional power plant [1], [2]. However, due to the inherent characteristics of randomness, intermittence and fluctuation of DGs, the secure and stable operation of the UG is threatened.

To adapt to the increasing penetration level of DGs and alleviate its side effects, the MG, which combines DGs, storage systems and interconnected loads, has extensively been examined. In general, the power quality (PQ) of the MG should be maintained at an acceptable level [3]. As for an MG operated in the grid-connected mode, the major PQ problems (PQPs) are dc injection, voltage fluctuations induced by DGs, overvoltage and current distortion, according to IEEE Std 1547-2018 (hereinafter referred to as the Standard) [4]. In this study, we focus on the last PQP mentioned. Thus, the total rated-current distortion (TRD) of the point of common coupling (PCC) must be constrained within 5% as required by the Standard.

The existing PQ improvement (PQI) methods can mainly be classified into two categories [5]. The first is to incorporate some traditional PQ conditioners in the MG, such as passive filters, active power filters (APFs) and static var generators (SVGs). However, the equipment requires extra investment in the cost of maintenance and operation. The other is to exploit the residual capacity (RC) of DGs for the PQP because the topology of a DG is the same as that of an APF, SVG, etc.

A DG embedded with a PQI function is also known as a multi-functional grid-tied inverter (MFGTI) [5]–[15]. Most of the existing research has concentrated on the topology [7], [8], controller [9], [10] and control objective [11], [12] of a single MFGTI, whereas little work has been done on the cooperation of multiple MFGTIs [13]–[15].

Due to the limited and variable RC, the PQP may not be handled thoroughly by a single MFGTI. Since there always exist several MFGTIs within an MG, it is appropriate to

coordinate all the MFGTIs to participate in the PQI task. A centralized control structure is proposed in [13], [14], where remote commands are transmitted to all the MFGTIs from the control centre. Then the active power injection reference for the power factor and adjustment of the level of harmonic compensation of MFGTIs are regulated according to the received commands. In [15], both the MFGTIs and loads are modelled as conductance and susceptance based on the Fryze-Buchholz-Depenbrock (FBD) theory. Then, by limiting the conductance and susceptance of MFGTI, the network conductance and susceptance are reshaped, and the harmonic and reactive current of the MG are shared among MFGTIs dispersedly. However, the compensation capacity is fixed regardless of the load condition, and the intrinsic nature of DGs is ignored. Thus, the utilization ratio of the RC is limited even under light load conditions [16].

With the rapidly increasing penetration ratio of DGs, the centralized schemes [13], [14] may not be suitable for its drawbacks [17]–[21]: reliability and security vulnerability of the central controller as a common point of failure, inadaptability to the plug and play requirement of an MG, etc. The decentralized method is also considered to be inappropriate for its inflexibility and waste of ready-made communication resources [15].

Therefore, a distributed control framework is needed to overcome the drawbacks of the centralized and decentralized methods and to adapt to the increasing number of MFGTIs. In fact, the distributed control strategies of MGs have widely been investigated [22]–[26]. In [22], the distributed cooperative control of multi-agent systems is firstly introduced to restore the voltage frequency and magnitude of the MG. Taking the practical communication network into consideration, a noise-resilient secondary controller is proposed in [23], [24] to deal with the additive type of noise and time-varying delay. However, most of the existing distributed control methods concentrate on the PQ of an islanded MG, but little work has been done on the PQ of a grid-tied MG based on distributed control theory. The difference is that the former focus on the voltage while the latter mainly concentrate on the current.

Based on the above analysis, a distributed control strategy is firstly proposed in this study for the grid-tied MG. It shares the PQI task among MFGTIs, which alleviates the drawbacks of the aforementioned centralized and decentralized methods [13]–[15] and makes full use of the RCs of the MFGTIs. In addition, the great majority of papers have concentrated on the PQP base on the assumption that the RC is sufficient. Little work has been done for the case where the RC is insufficient. To adapt to this scenario, a modified leader-follower consensus protocol is also proposed to decrease the active power injection of all MFGTIs to make room for the PQI task, where the decrement of the active power of all MFGTIs is proportional to their maximum available active power for fairness.

The main contributions of this paper are as follows:

1) A distributed control framework is incorporated in the PQI field to increase the reliability and flexibility of the proposed methods in the grid-tied scenario, which has not been done before to the best of the authors' knowledge.

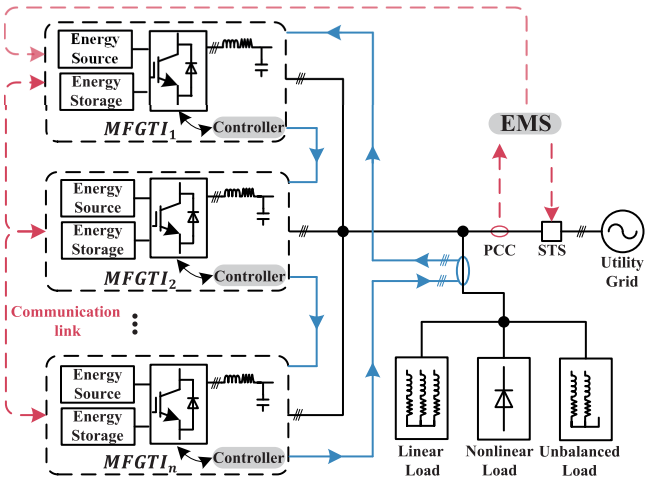

Fig. 1. Schematic of the MG architecture.

2) In the case of sufficient RC, a distributed consensus strategy is proposed to allocate the PQI task among the MFGTIs proportional to their instant RCs.
3) In the case of insufficient RC, a modified leader-follower consensus protocol is proposed to coordinate all the MFGTIs to scale down the active power outputs by the same factor to make room for the PQI task.
4) Different from the existing consensus methods, whose ultimate purpose is to ensure that all the agents converge to the same state for any initial state, the proposed methods aim at acquiring the initial states of the overall system. The convergence of states is an intermediate process of the proposed protocols.

The remainder of this paper is organized as follows: In Section II, some preliminaries and our control objects are presented. In Section III, the proposed methods for both sufficient and insufficient RC are given. The simulation results of the proposed methods are analyzed in Section IV. A hardware-in-the-loop experiment is presented in SectionV, which illustrates the effectiveness of the proposed algorithms under the plug-and-play scenario. Finally, Section VI concludes this paper.

II. Problem Formulation

A. Microgrid Structure

An MG consisting of multiple MFGTIs and typical loads is illustrated in Fig. 1.

The dc-link side of each MFGTI is denoted by an energy source and a storage system. A low-bandwidth communication system is required to implement the proposed distributed compensation strategy, and to enable each MFGTI to exchange information with its neighbours [27].

The local load comprises linear, nonlinear and unbalanced loads. Thus, the load current contains abundant harmonics and unbalanced components, which corrupts the PQ of the PCC and threatens the safe and stable operation of the MG. To fulfil the Standard, the load current is measured by current sensors and transmitted to n MFGTIs along the transmission path as shown by blue lines in Fig. 1. Then, the load current is measured and analyzed by the MFGTIs locally, and the

harmonic and unbalanced components are compensated by the MFGTIs according to their instant RCs that are defined in Section II-C.

In the case of insufficient RC, part of the harmonic and unbalanced currents will be injected into the PCC, which may deteriorate the PQ of the MG. To satisfy the Standard without introducing extra equipment, the output active power can be deliberately reduced according to the energy management system (EMS) to make room for the PQI task [4]. The detailed function of the EMS will be introduced in Section III-B.

B. Algebraic Graph Theory

A communication graph is a pair $\mathcal{G} = (\mathcal{E}, \mathcal{V})$ with $\mathcal{V} = \{v_1, \ldots, v_n\}$ being a set of N nodes and $\mathcal{E}$ a set of edges. Elements of $\mathcal{E}$ is denoted as $\{(v_j, v_i), if\ j \to i\}$ where $j \to i$ denotes that node i can receive information from node j.

Define the neighboring set of node i as $N_i \triangleq \{v_j \in \mathcal{V} | (v_j, v_i) \in \mathcal{E}\}$ with $|N_i|$ being the number of neighbors of node v_i. In an undirected graph, the distance between two nodes is the length of the shortest path connecting them. The greatest distance between any two nodes in $\mathcal{G}$ is named as the diameter $Diam\,\mathcal{G}$ of the graph.

Lemma 1 [28]: Consider a network of agents $x_i(k+1) = x_i(k) + u_i(k)$ with topology $\mathcal{G}$ applying the distributed consensus algorithm

$$u_i(k) = -\epsilon \sum_{j \in N_i} a_{ij} \left(x_i(k) - x_j(k)\right) \tag{1}$$

where $0 < \epsilon < \frac{1}{\Delta}$ and Δ is the maximum degree of the network. If the graph $\mathcal{G}$ is undirected, an average-consensus is asymptotically reached and the group decision value is $\alpha = \sum_{i=1}^{n} \frac{x_i(0)}{n}$.

Lemma 2 [29]: Consider a network of agents $x_i(k+1) = x_i(k) + u_i(k)$ with topology $\mathcal{G}$ applying the distributed consensus algorithm

$$u_i(k) = -T \sum_{j \in N_i} a_{ij} \left(x_i(k) - x_j(k)\right) - T a_{i0} \left(x_i(k) - x_0\right) \tag{2}$$

where x_0 denotes the leader node while x_i denotes the follower nodes. If node x_i can receive information from leader x_0, then $a_{i0} = 1$. Otherwise, $a_{i0} = 0$. T denotes the sampling period. If the leader has a directed path to all nodes and $T < min_{i=1,\ldots,n} \frac{1}{\sum_{j=0}^{n} a_{ij}}$, then all the states of follower nodes converge to the state of leader node ultimately: $x_i(k) = x_j(k) = x_0$.

C. Control Objectives

Although there still exist divergence in the decomposition of apparent power S, it is clear that S can be straightforwardly decomposed into two orthogonal quantities, active power P and nonactive power P_r [30], as illustrated in Fig. 2(a). The solid and dotted blue, orange and red lines denote P, P_r and S, respectively. At any time, one has $S^2 = P^2 + P_r^2$. It should be noted that for a given P, there exists a pair of P_r that leads or lags P by 90 degrees.

The capacity of the inverter can be either represented by the rated apparent power S or the root mean square (RMS) of the rated current I. Similar to the decomposition of S, I can be decomposed into active current I_a and nonactive current I_r. The RC is defined as the nonactive power P_r or current I_r.

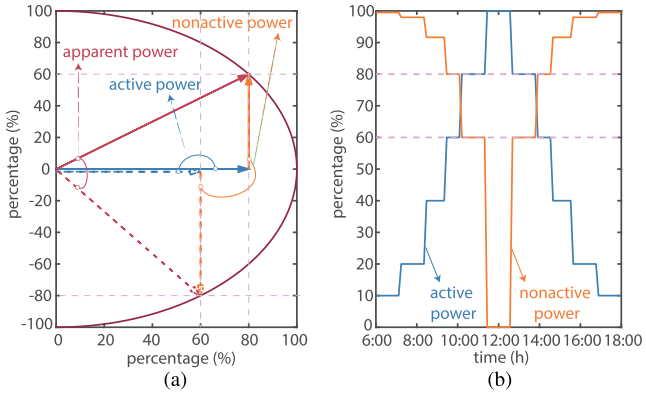

Fig. 2. Decomposition of apparent power. (a) Under ordinary case. (b) Under the solar power case of a sunny day.

$$P_r = \sqrt{S^2 - P^2} \quad \text{or} \quad I_r = \sqrt{I_s^2 - I_a^2} \tag{3}$$

Owing to the unfriendly nature of the renewable sources, the real-time active power output of a DG is variable. Taking solar power as an example and supposing that the sun rises at 6 a.m. and sets at 6 p.m., the maximum available active power of a sunny day can be like the blue line in Fig. 2. It is observed that although 80% of the rated power has been dispatched to deliver the active power at 10 a.m., there still exist 60% RC of the apparent power available, as illustrated in the orange line. If weak solar irradiance scenarios, such as rainy, cloudy days and a time after sunset are considered, there actually exists sufficient RC that has not been utilized. It is a similar case for wind power. Therefore, it is meaningful and economical if the aforementioned RC is fully exploited to participate in the PQI task, which leads to our first purpose.

Purpose 1: When the total RC is sufficient, the PQI task of the PCC is proportionally shared among n MFGTIs according to their individual RC I_{ri}. After compensation, the TRD of the PCC should be smaller than 5%.

The instantaneous current $i_{ci}(t)$ related to the PQI task can be written as follows:

$$i_{ci}(t) = \frac{I_{ri}}{\sum_{i=1}^{n} I_{ri}} \cdot i_{LC}(t) \tag{4}$$

where $i_{LC}(t)$ is part of load current that should be compensated, and $i_{ci}(t)$ is the reference current of $MFGTI_i$ associated with the PQP.

In this situation, sufficient RC means that the total RC of the MFGTIs is able to tackle the PQP of the MG. Because the sharing of the PQI task means an increase of RMS of the output current, it is fair to distribute the task among the MFGTIs proportionally.

When the renewable energy resources are abundant and the local load is heavy at the same time, the RC only may not be able to ensure that the TRD of the PCC fulfils the Standard. As mentioned in SectionII-A, it is suggested to reduce the active power output of each MFGTI to provide sufficient RC for the PQI task. Because the active power generation is the

main benefit of each MFGTI, it is required to decrease the active power reference proportionally.

Thus, our second purpose is described as follows:

Purpose 2: When the RC is insufficient, the real-time active power output of $MFGTI_i$ is no longer the same as the MPPT, but multiplied by an appropriate factor β $(0 < \beta < 1)$. The factor should be the same for all the MFGTIs and promises that there exist sufficient RC to deal with the PQP. Besides, the PQI task should be proportionally shared among the MFGTIs. After compensation, the TRD of the PCC should be smaller than 5%.

The main difficulty of purpose 1 and 2 is how to acquire the denominator of (4) and obtain a suitable β, which is dealt with under the distributed control framework in the following sections.

III. Proposed Distributed Consensus Methods

A. Distributed Consensus Method for the Case With Sufficient RC

For the microgrid shown in Fig. 1, denote the actual RC I_{ri} of $MFGTI_i$ as x_{ri} and assign a virtual state x_{vi} for $MFGTI_i$, where actual state means that x_{ri} is a physical quantity, while virtual state means that x_{vi} is an artificial one. x_{vi} is adopted in this study because only information consensus is needed to achieve our purposes.

Assumption 1: The changing rate of x_{vi} is much larger than that of x_{ri}. Thus, x_{ri} can be seen as a constant during two successive changing moments compared with x_{vi}.

Because the time scale of inverter dynamics is much smaller than the change of renewable energy, assumption 1 is reasonable. In a mathematical representation, supposing that x_{ri}, for $i = 1, \ldots, n$, changes at some discrete-time instants $t = t_m^i$, for $m \in \mathbb{N}$, then time t can be split and represented as $t = \cup_{m=0}^{\infty} \left[t_m^i, t_{m+1}^i\right)$, where $\left[t_m^i, t_{m+1}^i\right) = \cup_{h=0}^{n_m} \left[t_m^i + hT, t_m^i + hT + 1\right)$, for $h \in \mathbb{N}$, [2], [31]. The split of time t is illustrated in Fig. 3(b) and will be explained in detail later.

Under the above definition and assumption 1, $x_{ri}(kT)$ holds constant, which means $x_{ri}\,(kT) = x_{ri}\left(t_m^i\right)$, during $t_m^i \leqslant kT < t_{m+1}^i$, for $k \in \mathbb{N}$. To simplify the denotation, k is short for kT in the following context.

For a given positive constant ε_i, let's define $\gamma_i(k)$ as

$$\gamma_i\,(k) = \begin{cases} 1, & |x_{ri}\,(k) - x_{ri}\,(k-1)\,| > \varepsilon_i \\ 0, & otherwise \end{cases} \tag{5}$$

To fulfil purpose 1, we propose the following distributed consensus method

$$x_{vi}\,(k) = \begin{cases} x_{ri}\,(k), & \gamma_i\,(k) = 1 \ or \ \sum_{j\in N_i} \gamma_j\,(k) \geqslant 1 \\ x_{vi}\,(k-1) + u_i, & otherwise \end{cases} \tag{6}$$

where $u_i = -c_i \sum_{j\in N_i} \left[x_{vi}\,(k-1) - x_{vj}\,(k-1)\right]$, γ_j and x_{vj} are the neighboring information transmitted to $MFGTI_i$, c_i is a convergence coefficient.

Theorem 1: For a MG shown in Fig.1, the residual capacity of $MFGTI_i$ is denoted as $x_{ri}(k)$ and the harmonic and unbalanced current of the load is represented as $i_{LC}(k)$. In the case of sufficient residual capacity, i.e. $\sum_{i=1}^{n} ||x_{ri}(k)|| \geq ||i_{LC}(k)||$, $i_{LC}(k)$ can be proportionally shared among MFGTIs according to their residual capacities under the proposed distributed protocol (5)(6) and Algorithm 1. To be specific, the instantaneous current $i_{ci}(k)$ related to the PQI task can be written as $i_{ci}(k) = \frac{I_{ri}(k)}{n \cdot x_{vi}(k)} \cdot i_{LC}(k)$.

Algorithm 1 Proposed Consensus Protocol (5, 6) of Agent i

Input: $x_{ri}(k)$, $x_{ri}(k-1)$, $x_{vi}(k-1)$, $\gamma_j(k)$ and $x_{vj}(k-1)$ for $j \in N_i$

Output: $x_{vi}(k)$, $\gamma_i(k)$

```
Given parameters c_i, ε_i and positive integer N. Set Cnt = 0, γ_i(0) = 1, flag = 0.
while (1) do
  if |x_ri(k) − x_ri(k−1)| > ε_i then
      γ_i(k) = 1.   flag = 1.
  end if
  if γ_i(k) == 1 or Σ_{j∈N_i} γ_j(k) ⩾ 1 then
    if Cnt < N then
      γ_i(k) = 1.   flag = 0.   Cnt = Cnt + 1.
    else
      if flag == 1 then
          γ_i(k) = 1.   flag = 0.
      else
          γ_i(k) = 0.
      end if
    end if
  else
    Cnt = 0.
  end if
  if γ_i(k) = 1 then
    x_vi(k) = x_ri(k).
  else
    u_i(k) = −c_i Σ_{j∈N_i} (x_vi(k−1) − x_vj(k−1)).
    x_vi(k) = x_vi(k−1) + u_i(k).
  end if
end while
```

Proof: The proposed protocol (5) and (6) can be interpreted as that the virtual state x_{vi} will be reset to the actual RC x_{ri} whenever x_{ri} or x_{rj}, for $j \in N_i$, changes. If all the x_{ri}, for $i = 1, \ldots, n$, enter into the steady state, the protocol (6) degrades into the traditional form (1).

According to Lemma 1, one can derive that

$$\begin{aligned} \lim_{k\to t_{m+1}^i} x_{vi}\,(k) &= \sum_{j=1}^{n} \frac{x_{vj}\left(t_m^i\right)}{n} = \sum_{j=1}^{n} \frac{x_{rj}\left(t_m^i\right)}{n} \\ &= \frac{1}{n} \sum_{j=1}^{n} x_{rj}\,(k), \quad for \ t_m^i \leqslant k < t_{m+1}^i \end{aligned} \tag{7}$$

The last equation of (7) shows that the denominator of (4) can be derived with the proposed distributed protocol (5) and (6). The only requirement is that the length of the time interval $[t_k^i, t_{k+1}^i)$ is larger than that of the convergence time of x_{vi}. Considering the larger time scale of x_{ri} and the acceptable convergence precision, this requirement can be fulfilled with a proper designed c_i.

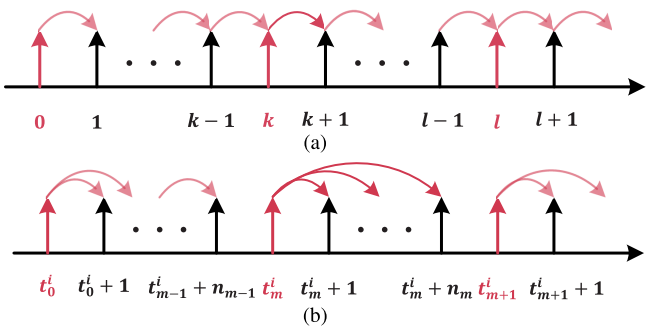

Fig. 3. Time division. (a) Under protocol (1). (b) Under protocol (5, 6).

Therefore, (4) can be transformed into

$$i_{ci}(k) = \frac{I_{ri}(k)}{\sum_{i=1}^{n} I_{ri}} \cdot i_{LC}(k) = \frac{I_{ri}(k)}{n \cdot x_{vi}(k)} \cdot i_{LC}(k) \tag{8}$$

where only the neighboring information is needed in (7, 8).

Therefore, with $i_{ci}(k)$ calculated as (8), $i_{LC}(k)$ can be proportionally shared among MFGTIs according to their residual capacities.

This concludes the proof. ■

Algorithm 1 is given to explain the detailed procedures of the proposed protocol (5, 6). Step $3-5$ is named as the self-triggered condition. $\gamma_i(k)$ is an enable bit adopted to decide whether to assign the value of $x_{ri}(k)$ to $x_{vi}(k)$ or not, as shown in step $19-24$. Step $6-8$ is called the broadcasting period during which any arrival of the self-triggered condition of agent i will broadcast to all the agents within N sampling periods. Thus, it is required that N should be set to be larger than the diameter of the communication graph. Step $10-14$ is referred to as the restraining period. During this period, all the $\gamma_i(k)$ is reset to zero except for one instant when self-triggered condition is satisfied. After this period, the whole system is prepared for the next broadcasting and restraining phase. If $x_{ri}(k)$, for $i = 1, \ldots, n$, and $x_{rj}(k)$, for $j \in N_i$, hold the same value, $x_{vi}(k)$ will converge to $\sum_{i=1}^{n} x_{ri}(k)/n$ under step $22-23$.

It should be noted that only step $22-23$ is needed to realize protocol (1), which is different from the proposed protocol (5) and (6).

There is another perspective which can describe the difference between the proposed protocol (5, 6) and protocol (1). That is how they deal with the time t, as shown in Fig. 3.

As for protocol (1), t is evenly divided and the time interval is equal to the sampling time T. Thus, t is arranged as $t = \cup_{k=0}^{\infty}[k, k+1)$. For the system state $x_i(k)$, for $i = 1, \ldots, n$, at any instant $t = k$, $x_i(k-1)$ can be seen as the initial state of agent i, as illustrated in Fig. 3(a).

However, as described before, t is split and represented as $t = \cup_{m=0}^{\infty}\left[t_m^i, t_{m+1}^i\right)$ under protocol (5, 6). In this study, our purpose is to deduce the sum of $x_{ri}(t_m^i)$, for $t \in \left[t_m^i, t_{m+1}^i\right)$. In other words, it is required that $x_{vi}(k)$, for $k \in \left[t_m^i, t_{m+1}^i\right)$, converges to $\sum_{i=1}^{n} x_{ri}(t_m^i)/n$. Thus, the initial state of $x_{vi}(k)$, for $k \in \left[t_m^i, t_{m+1}^i\right)$, is $x_{ri}(t_m^i)$ rather than $x_{vi}(k-1)$, as illustrated by pink arrows in Fig. 3(b).

With Theorem 1, our Purpose 1 can be fulfilled.

Algorithm 2 Proposed Consensus Protocol (12) of Agent i

Input: $P_{Mi}(k)$, $v_{di}(k)$, $x_{ri}(k-1)$, $x_{vi}(k-1)$, $\beta_i(k-1)$, $\beta_0(k-1)$; $\beta_j(k-1)$, $\gamma_j(k)$ and $x_{vj}(k-1)$ for $j \in N_i$

Output: $P_i^*(k)$, $x_{vi}(k)$, $\gamma_i(k)$

Given parameters $I_{Ni}, c_i, c_{\beta i}, a_{i0}, c_{\beta 0 i}, \varepsilon_i$ and positive integer N. Set $Cnt = 0$, $\gamma_i(0) = \beta_i(0) = 1$, $flag = 0$.
while (1) **do**
  $u_{\beta i}(k) = -c_{\beta i} \sum_{j \in N_i} \left[\beta_i(k-1) - \beta_j(k-1)\right]$.
  $u_{\beta 0 i}(k) = -c_{\beta 0 i} \cdot a_{i0} \left[\beta_i(k-1) - \beta_0(k-1)\right]$.
  $\beta_i(k) = \beta_i(k-1) + u_{\beta i}(k) + u_{\beta 0 i}(k)$.
  if $\beta_i(k) > 1$ **then**
    $\beta_i(k) = 1$.
  else
    if $\beta_i(k) < 0$ **then**
      $\beta_i(k) = 0$.
    end if
  end if
  $P_i^*(k) = \beta_i(k) \cdot P_{Mi}(k)$.
  $I_{di}(k) = 2P_i^*(k)/(3v_{di}(k))$.
  $x_{ri}(k) = \sqrt{I_{Ni}^2 - I_{di}^2(k)/2}$.
  The rest is the same as Step $3-24$ of Algorithm 1.
end while

B. Leader-Follower Consensus Method for the Case With Insufficient RC

Although algorithm 1 is able to ensure that the PQI task is shared among the MFGTIs according to their instant RC, it requires a prior assumption—sufficient RC, which means $\sum_{i=1}^{n} ||x_{ri}(k)|| \geqslant I_{LC}(k)$. This condition promises

$$||i_{ri}(k)|| = ||\frac{I_{ri}(k)}{\sum_{i=1}^{n} I_{ri}(k)} \cdot i_{LC}(k)|| \leqslant I_{ri}(k) \tag{9}$$

This assumption is not always appropriate, especially when the renewable energy resources are abundant. If $||i_{ri}(k)|| > I_{ri}(k)$, the sharing coefficients can be chosen as $\frac{I_{ri}(k)}{||i_{LC}(k)||}$ to prevent overcurrent. Thus,

$$||i_{ri}(k)|| = ||\frac{I_{ri}(k)}{||i_{LC}(k)||} \cdot i_{LC}(k)|| = I_{ri}(k) \tag{10}$$

In this situation, each MFGTI has participated in the PQI task to the best of their abilities. However, because $\sum_{i=1}^{n} I_{ri}(k) < I_{LC}(k)$, part of the nonactive current of the nonlinear load will inject into the PCC, which may lead to $TRD_{PCC} > 5\%$.

Traditionally, one can either cut down some unimportant loads or put in additional PQ conditioners to deal with this problem. However, it's hard to decide which load is unimportant. And additional equipment asks for extra investment and reconfiguration of the hardware. Therefore, a modified algorithm based on regulating the active power is proposed in this section.

The EMS, as shown in Fig. 1, can calculate the TRD of the PCC current. Although the Standard only requires that $TRD \leq 5\%$, we choose to set $TRD^r = 2\%$ rather than 5% for a better PQ performance at the sacrifice of lower active power output.

The following function is assigned to the EMS.

$$\beta_0(k) = \beta_0(k-1) + k_p(TRD^r - TRD(k)) \tag{11}$$

where $k_p > 0$ is a given gain.

$\beta_0(k)$ is transmitted to any MFGTI that can receive information from the EMS, for example $MFGTI_1$ as shown in Fig. 1. A leader-follower consensus protocol is then proposed to regulate the active power output P_i of $MFGTI_i$.

$$\begin{aligned}\beta_i(k) = \beta_i(k-1) - c_{\beta i}\sum_{j\in N_i}\left[\beta_i(k-1) - \beta_j(k-1)\right] \\ -c_{\beta 0i}\cdot a_{i0}\left[\beta_i(k-1) - \beta_0(k-1)\right]\end{aligned} \tag{12}$$

where $c_{\beta i}$ and $c_{\beta 0i}$ are positive proportional coefficients. $a_{i0} = 1$ if $MFGTI_i$ can receive information from EMS and $a_{i0} = 0$, otherwise.

The active power reference P_i^* is then modified as

$$P_i^*(k) = \beta_i(k)\cdot P_{Mi}(k) \tag{13}$$

where $P_{Mi}(k)$ is the maximum power point of $MFGTI_i$.

The residual capacity $x_{ri}(k)$ is modified as

$$x_{ri}(k) = \sqrt{I_{Ni}^2 - I_{di}^2(k)/2} \tag{14}$$

where I_{Ni} is the rated phase current and

$$I_{di}(k) = 2P_i^*(k)/(3v_{di}(k)) \tag{15}$$

where $v_{di}(k)$ is the voltage magnitude on d axis.

Theorem 2: For a MG shown in Fig.1, the residual capacity of $MFGTI_i$ is denoted as $x_{ri}(k)$ and the harmonic and unbalanced current of the load is represented as $i_{LC}(k)$. In the case of insufficient residual capacity, i.e. $\sum_{i=1}^{n}||x_{ri}(k)|| < ||i_{LC}(k)||$, the active power output of $MFGTI_i$ can be scaled down by a same factor $\beta_i(k) = \beta_0(k)$, for $i = 1,\ldots,n$, determined by (11) and (12). Then, part of $i_{LC}(k)$ can be proportionally shared among MFGTIs according to their instant residual capacities. The regulation process of $\beta_i(k)$ will not stop until $TRD(k) = TRD^r$, i.e. $TRD(k) = 2\%$. Finally, $i_{LC}(k)$ can be fully shared among MFGTIs according to Algorithm 2.

Proof: Firstly, it should be mentioned that the sampling period of β_0 is much larger than $\beta_i, i = 1, 2, \ldots n$. According to Lemma 2, β_i can gradually converge to β_0 at the steady state. After β_i settles down, the residual capacity of $MFGTI_i$ is calculated according to (13), (14) and (15). Then, Algorithm 2 degrades into Algorithm 1. With Theorem 1, Theorem 2 is proven. ■

The detailed realization of the proposed method is presented in Algorithm 2.

With Theorem 2, our Purpose 2 can be fulfilled under this algorithm.

IV. Simulation Results

To test the feasibility of the proposed consensus methods, simulations based on the MG of Fig. 1 have been implemented through MATLAB/Simulink, where $n = 3$ is adopted for illustration. The system parameters are listed as follows.

1) The system voltage is 380 V (RMS, line-to-line), 50Hz.
2) The apparent power of MFGTI is 10 kVA. The LCL filter is designed as: converter-side inductor $L_g = 1\,mH$, grid-side inductor $L_o = 40\,\mu H$, filter capacitor $C = 30\,\mu F$. The switching and sampling frequency is $10\,kHz$, $20\,kHz$, respectively.
3) The control parameters of algorithm 1: $c_i = 0.01$, $\varepsilon_i = 0.005$, $N = 4$. The sampling period of the consensus protocol (5) and (6) is 1 ms.
4) The control parameters of algorithm 2: $c_i = 0.03$, $\varepsilon_i = 0.005$, $N = 20$, $c_{\beta i} = c_{\beta 0i} = 0.4$. The sampling period of the consensus protocol (11) is 150 ms while that of (12) is 1 ms.

A. Effectiveness of the Proposed Method Under Sufficient Residual Capacity

In this section, to ensure sufficient RC of the MG, the maximum available active power of each MFGTI is set to be less than 80% of the rated power S. To reflect the stochastic characteristic of renewable energy, the MPPT of each MFGTI is arbitrarily defined as shown in Fig. 5(a), where the low-frequency variation of MPPT represents the larger time scale of fluctuation of renewable energy compared with the inverter dynamics.

The local load consists of linear, nonlinear and unbalanced load and is connected to the UG at the start of the simulation. Before $t = 0.1s$, only local loads are connected to the UG. The harmonic and unbalance current injected totally into the PCC, as shown in Fig. 5(d). The TRD of this period is nearly 20% according to Fig. 5(f).

During $t \in [0.1s, 0.15s)$, MFGTIs are connected to the UG and the active power reference is 5kW, as shown in Fig. 5(a). Because part of the active power component of the load current is supplied by MFGTIs, the TRD of the PCC further deteriorated to almost 60% according to Fig. 5(f).

After $t = 0.15s$, the harmonic and unbalanced components of load current are calculated and shared among MFGTIs proportionally. As illustrated in Fig. 5(c), X_{vi} converges to the average value of RCs under the proposed protocol (5, 6) and algorithm 1, whenever the RC of any MFGTI changes. The sharing ratio of MFGTI is derived according to the ratio of their RC, whose regulation process is presented in Fig. 5(e). The sum of the sharing ratio of MFGTIs is denoted by purple dotted lines in Fig. 5(e). It should be noted that the sum of the ratios is multiplied by 0.2 to make the figure more compact. Therefore, the PQI task has been fully shared among MFGTIs because the sum of the ratios is equal to one.

The PCC current during the whole regulation process is shown in Fig. 5(b). The regulation process during $t \in [0.06s, 0.2s)$ is given in Fig. 5(d). The PQ of the PCC has been improved according to the current waveform during $t \in [0.16, 0.2]$, which is nearly sinusoidal. The TRD of the PCC is illustrated in Fig. 5(f). After compensation, the TRD has been decreased smaller than 5%, except for some critical instants when the MPPT of any MFGTI changes. The abrupt change of TRD shown in Fig. 5(f) is inevitable and acceptable.

According to the above analysis, it can be concluded that purpose 1 has been achieved under the proposed protocol (5, 6) and algorithm 1.

B. Effectiveness of the Proposed Method Under Insufficient Residual Capacity

In this section, the MPPT of MFGTIs is set to be constant, as shown in Fig. 4(a). Due to the active power references of

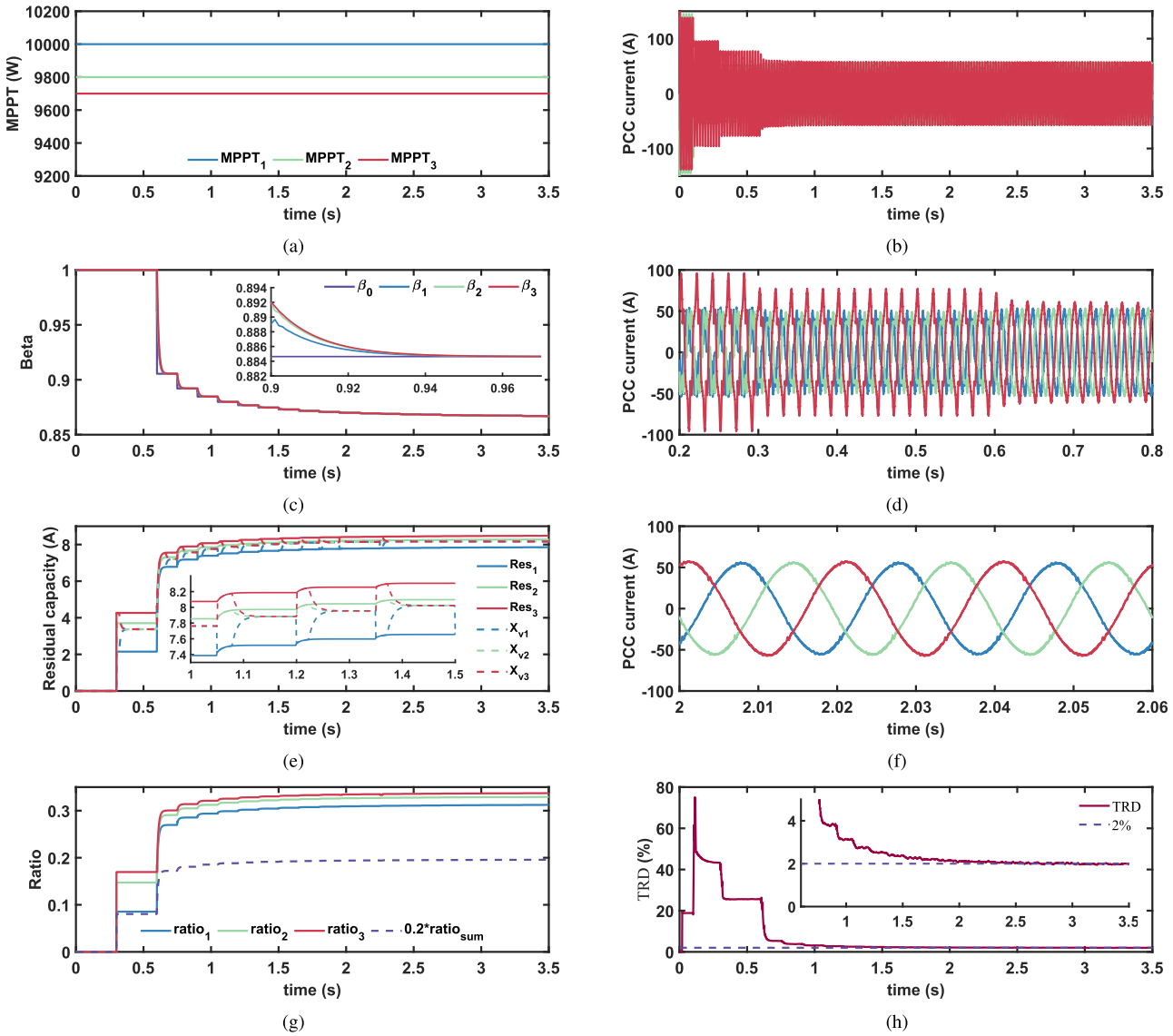

Fig. 4. Regulation process under algorithm 2 with $TRD^r = 2\%$. (a) Variation of MPPT. (b) PCC current during whole simulation. (c) Scaled factor β_i related to active power reference P_i^*. (d) PCC current during $t \in [0.2s, 0.8s]$. (e) Residual capacity and consensus of x_{vi}. (f) PCC current during $t \in [2s, 2.06s]$. (g) Sharing ratio of power quality improvement task of $MFGTI_i$. (h) TRD of the PCC current.

MFGTIs having approached their rated power, the available RC is insufficient to deal with the PQP.

During $t \in [0.1s, 0.3s)$, only the active power of $MFGTI_i$ is generated according to MPPT, and the TRD of this time interval is 40%, as presented in Fig. 4(h). During $t \in [0.3s, 0.5s)$, all the MFGTIs have participated in the PQI task. Fig. 4(d) shows that the instantaneous value of the unbalanced current has been decreased compared with $t \in [0.2s, 0.3s)$. From Fig. 4(e), it can be observed that x_{vi} is able to converge to the average value of RCs. However, because the RC is insufficient, the sum of the ratios is smaller than one during $t \in [0.3s, 0.5s)$, as illustrated in Fig. 4(g). To be specific, only nearly 50% of the harmonic and unbalanced currents have been shared. Nevertheless, the TRD has decreased from 40% to nearly 20% as shown in Fig. 4(h).

At $t = 0.5s$, the EMS starts to measure the TRD of the PCC. Then, β_0 is calculated according to (11) and transmitted to $MFGTI_1$. β_i, for $i = 1, 2, 3$, is updated according to (12) and algorithm 2. With the renewed β_i, the active power reference is no longer equal to the MPPT, but calculated according to (13). It should be noted that the sampling time of β_0 is 150 ms while that of β_i, for $i = 1, 2, 3$, is 1 ms.

The regulation process of β_i is illustrated in Fig. 4(c). It shows that with the leader-follower consensus protocol (12), β_i is able to track the reference β_0 given by the PCC. The final value of β_i is nearly 0.87, as shown in Fig. 4(c).

Due to the active power of $MFGTI_i$ having been decreased, its RC increases. Then, x_{vi} converges to the new value according to algorithm 2, as shown in Fig. 4(e). At the same time, the sharing ratio of MFGTIs increases accordingly.

The PCC current of the whole regulation process is given in Fig. 4(b), and Fig. 4(f) illustrates the waveform of the load current during $t \in [2s, 2.06s)$. According to Fig. 4(h), the TRD has decreased to 2% during $t \in [2s, 3.5s)$, which fulfils the requirement of the Standard.

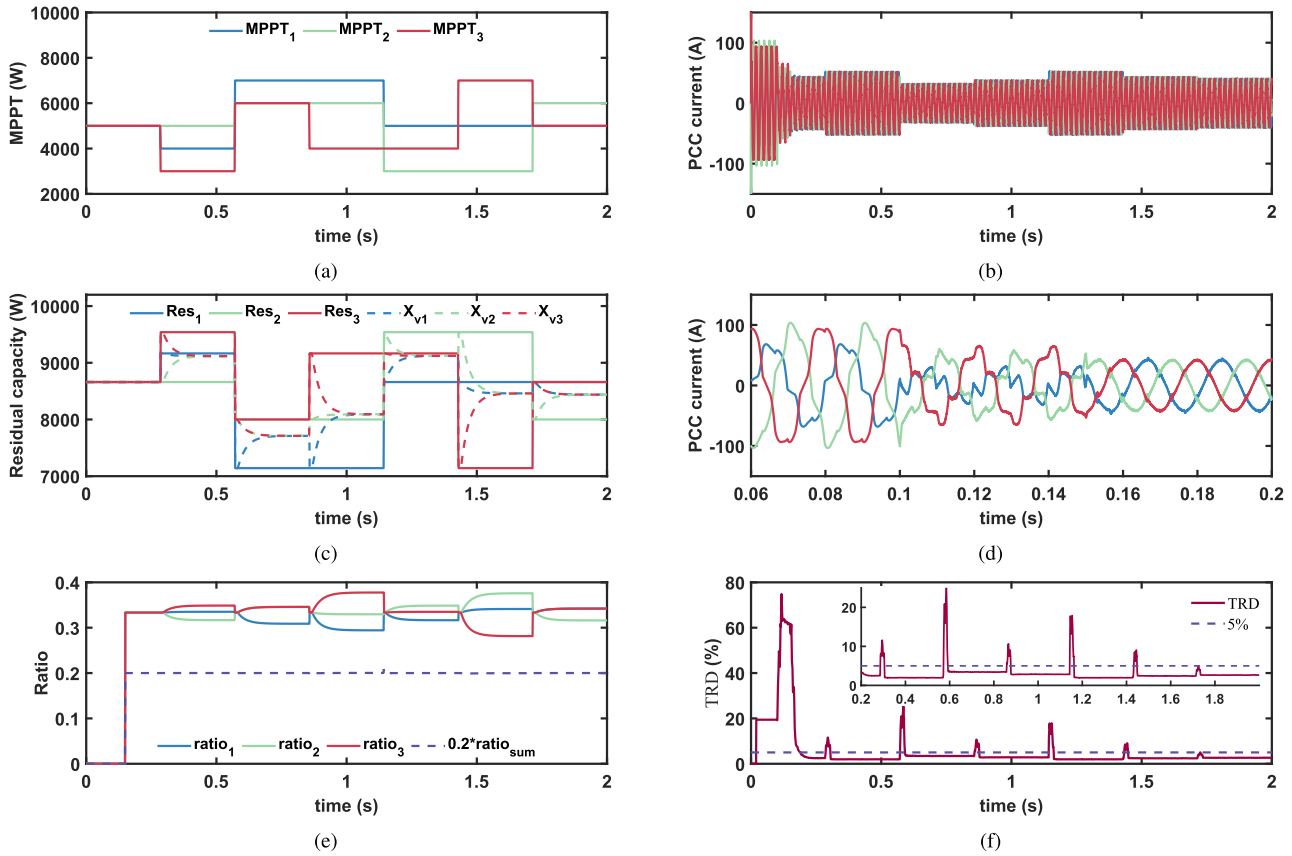

Fig. 5. Regulation process under algorithm 1. (a) Variation of MPPT. (b) PCC current during whole simulation. (c) Residual capacity and consensus of x_{vi}. (d) PCC current during $t \in [0.06s, 0.2s]$. (e) Sharing ratio of power quality improvement task of $MFGTI_i$. (f) TRD of the PCC current.

According to the above analysis, it can be concluded that purpose 2 has been achieved under the proposed protocol (11) and (12) and algorithm 2.

V. Experimental Results

To further illustrate the effectiveness of the proposed methods, hardware-in-the-loop (HIL) experiments have been performed based on the platform shown in Fig.7. The system parameters are the same as that in Section IV.

The OP5700 is a flagship real-time digital simulator of OPAL-RT and combines the power of a Xilinx Virtex-7 FPGA with up to 32 of the latest Intel Xeon processing cores. The main topology of the microgrid is programmed in the FPGA through eHSx128 Gen3 block. Some auxiliary blocks are established in RTLAB v11.3.6, together with Matlab 2016b, to control the communication of the FPGA with CPU and DSP. The main algorithm is programmed in the OP8665, where TMS320F28335 functions as the main controller. The experimental results are recorded by Yokogawa DL350.

Due to the space limitation, only the plug-and-play scenario is presented to verify the feasibility of the proposed method under insufficient residual capacity in this section, where $MFGTI_3$ is disconnected from the MG and then reconnected.

The regulation process of β_i is shown in Fig. 6(a), where CH1_1, CH1_2, CH2_1 and CH2_2 denote β_0, β_1, β_2 and β_3, respectively. Before compensation, the active power output of MFGTIs is the same as their MPPTs, and thus β_i is equal to one. After the compensation function is enabled, β_0 is regulated according to equation (11) and $\beta_{1,2,3}$ converge to β_0 under the algorithm 2. The steady value of β_i is 0.86, which is similar to the result of 4(c). After $MFGTI_3$ is disconnected from the MG, β_3 is reset to 1. The compensation task is therefore shared among $MFGTI_1$ and $MFGTI_2$. To fulfill the Standard, the active power of $MFGTI_i, i = 1, 2$ further decreases. After $MFGTI_3$ is reconnected, β_3 converges to β_0. The convergence value is 0.838, which is almost the same as that before $MFGTI_3$ is reconnected. It is reasonable because with only the residual capacity of $MFGTI_i, i = 1, 2$, the TRD of PCC has been controlled under 2%, let alone $MFGTI_3$ joins in. However, since the load does not change in this scenario, the proper value of β_i is 0.86. The difference between 0.86 and 0.838 means that each MFGTI has the potential to provide more active power while promise the fulfillment of the Standard. Therefore, we introduce a resetting process. Whenever the MFGTI is connected or reconnected to the MG, β_0 is reset to one. Then, β_i will converge to the proper value as illustrated in Fig.6(a).

The regulation process of X_{vi} and Res_i is shown in Fig. 6(b), where CH1_1, CH1_2, CH2_1, CH2_2, CH3_1 and CH3_2 denote X_{v1}, X_{v2}, X_{v3} and Res_1, Res_2, Res_3, respectively. After the compensation function is activated, the residual capacity of MFGTIs is calculated, and then X_{vi} converges to the average value of $Res_i, i = 1, 2, 3$. The regulation process is the same as that in Fig.4(e). After $MFGTI_3$ is disconnected, its residual capacity is set to be zero. Since $\beta_i, i = 1, 2$ decreases, their residual capacities increase and

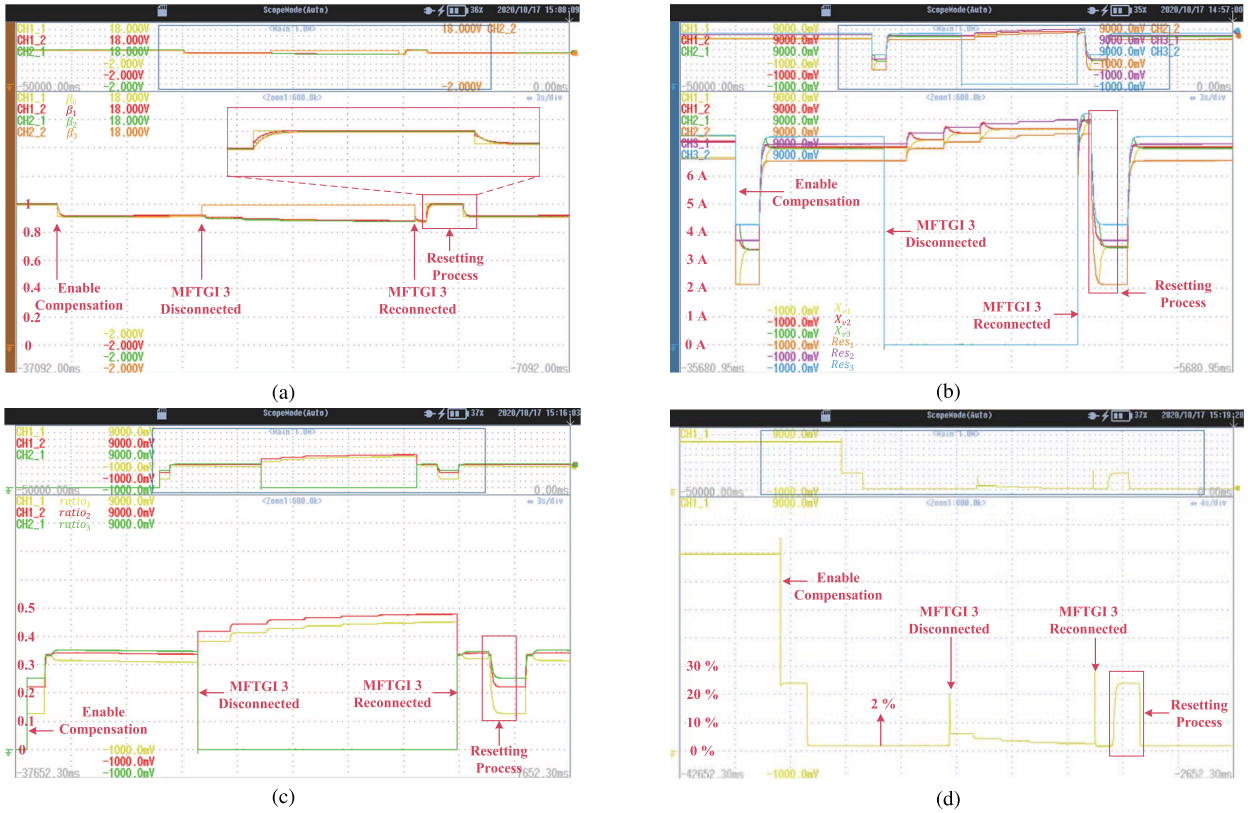

Fig. 6. Experimental regulation process of algorithm 2 under the plug-and-play scenario. (a) Scaled factor β_i related to active power reference P_i^*. (b) Residual capacity and consensus of x_{vi}. (c) Sharing ratio of power quality improvement task of $MFGTI_i$. (d) TRD of the PCC current.

$X_{vi}, i = 1, 2$ can effectively converge to the average value under the proposed algorithm 2. After the reconnection of $MFGTI_3$ and the resetting process, X_{vi} converges to the proper value before $MFGTI_3$ is disconnected.

The regulation process of $ratio_i$ is shown in Fig. 6(c), where CH1_1, CH1_2 and CH2_1 denote $ratio_1, ratio_2$ and $ratio_3$, respectively. Before the MFGTIs participate in the compensation task, their sharing ratio is zero. After the compensation function is enabled, $ratio_i$ increases according to their RCs. Since Res_1 is the smallest as shown in Fig.6(b), $MFGTI_1$ has the fewest RC to undertake the compensation task. Thus, $ratio_1$ is the smallest one as shown in Fig.6(c). After $MFGTI_3$ is disconnected from the MG, The sharing ratio of $MFGTI_1$ and $MFGTI_2$ increases to fulfill the Standard. The sum of $ratio_1$ and $ratio_2$ is slightly smaller than one because the TRD of PCC has already been controlled under 2%. After the reconnection of $MFGTI_3$ and the resetting process, the sharing ratio of the compensation task converges to the value before $MFGTI_3$ is disconnected.

The regulation process of the indicator of whether the PQP has been tackled, i.e. TRD, is shown in Fig. 6(d). After the compensation function is activated, TRD decreases to 24% in a short time and then regulated to 2%, where $TRD^r = 2\%$, rather than $TRD^r = 5\%$, is chosen for a better PQ. The regulation process is similar to that in Fig.4(h). After $MFGTI_3$ is disconnected from the MG, TRD sharply increases to 20% and then gradually decreases to 2%. The PQ of the PCC is ensured after the reconnection of $MFGTI_3$ and the resetting process.

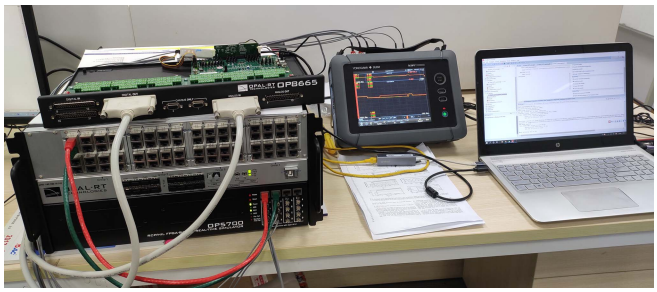

Fig. 7. Experimental setup.

The above experimental results and analysis verify that the proposed methods is effective, even under the plug-and-play scenario.

VI. Conclusion

This paper concentrates on the cooperative sharing of the PQI task of the MG. The distributed control framework is firstly introduced in the PQI field regarding the grid-tied scenario. Different from the existing consensus methods, whose ultimate purpose is to ensure that all the agents converge to the same state for any initial state, the proposed methods aim at acquiring the initial states of the overall system, and the convergence of states is an intermediate process of the proposed protocols.

To fairly allocate the PQI task, the sharing ratio of each MFGTI is derived according to the ratio of its RC to the whole RC of all the MFGTIs. As for the case of sufficient RC, a distributed consensus method is proposed to approximate the

whole RC with the only neighbouring information exchange. For the scenario of insufficient RC, the active power injection of MFGTI is scaled down by the same factor, which is realized by a leader-follower method, to make room for the PQI task. Simulations and a hardware-in-the-loop experiment of an MG consisting of three MFGTIs, are carried out and verify that under the proposed methods, the PQI task is fairly allocated among MFGTIs, and the PQ of the PCC fulfils the IEEE Std 1547-2018.

In this paper, only the basic consensus method is adopted. Our future work will concentrate on the combination with the finite-time consensus method and event-triggered mechanism.

REFERENCES

[1] H. Yan, J. Han, H. Zhang, X. Zhan, and Y. Wang, "Adaptive event-triggered predictive control for finite time microgrid," *IEEE Trans. Circuits Syst. I, Reg. Papers*, vol. 67, no. 3, pp. 1035–1044, Mar. 2020.

[2] S. Hu, P. Yuan, D. Yue, C. Dou, Z. Cheng, and Y. Zhang, "Attack-resilient event-triggered controller design of DC microgrids under DoS attacks," *IEEE Trans. Circuits Syst. I, Reg. Papers*, vol. 67, no. 2, pp. 699–710, Feb. 2020.

[3] M. N. Kabir, Y. Mishra, G. Ledwich, Z. Y. Dong, and K. P. Wong, "Coordinated control of grid-connected photovoltaic reactive power and battery energy storage systems to improve the voltage profile of a residential distribution feeder," *IEEE Trans. Ind. Informat.*, vol. 10, no. 2, pp. 967–977, May 2014.

[4] *IEEE Standard for Interconnection and Interoperability of Distributed Energy Resources With Associated Electric Power Systems Interfaces*, IEEE Standard 1547-2018 (Revision IEEE Std 1547-2003), Apr. 2018, pp. 1–138.

[5] Z. Zeng, H. Yang, J. M. Guerrero, and R. Zhao, "Multi-functional distributed generation unit for power quality enhancement," *IET Power Electron.*, vol. 8, no. 3, pp. 467–476, Mar. 2015.

[6] J. Chen, D. Yue, X. Shao, and S. Bai, "Control strategy for multi-functional grid-tied inverters based on conservative power theory," in *Proc. 37th Chin. Control Conf. (CCC)*, Jul. 2018, pp. 8904–8908.

[7] W. Choi, W. Lee, D. Han, and B. Sarlioglu, "New configuration of multifunctional grid-connected inverter to improve both current-based and voltage-based power quality," *IEEE Trans. Ind. Appl.*, vol. 54, no. 6, pp. 6374–6382, Nov. 2018.

[8] J. Wang, K. Sun, H. Wu, L. Zhang, J. Zhu, and Y. Xing, "Quasi-two-stage multifunctional photovoltaic inverter with power quality control and enhanced conversion efficiency," *IEEE Trans. Power Electron.*, vol. 35, no. 7, pp. 7073–7085, Jul. 2020.

[9] T. Ye, N. Dai, C.-S. Lam, M.-C. Wong, and J. M. Guerrero, "Analysis, design, and implementation of a quasi-proportional-resonant controller for a multifunctional capacitive-coupling grid-connected inverter," *IEEE Trans. Ind. Appl.*, vol. 52, no. 5, pp. 4269–4280, Sep. 2016.

[10] A. S. Bubshait, A. Mortezaei, M. G. Simoes, and T. D. C. Busarello, "Power quality enhancement for a grid connected wind turbine energy system," *IEEE Trans. Ind. Appl.*, vol. 53, no. 3, pp. 2495–2505, Jun. 2017.

[11] Z. Zeng, H. Yang, S. Tang, and R. Zhao, "Objective-oriented power quality compensation of multifunctional grid-tied inverters and its application in microgrids," *IEEE Trans. Power Electron.*, vol. 30, no. 3, pp. 1255–1265, Mar. 2015.

[12] Z. Zeng, H. Li, R. Zhao, S. Tang, and H. Yang, "Multi-objective control of multi-functional grid-connected inverter for renewable energy integration and power quality service," *IET Power Electron.*, vol. 9, no. 4, pp. 761–770, Mar. 2016.

[13] H. K. Morales-Paredes, J. P. Bonaldo, and J. A. Pomilio, "Centralized control center implementation for synergistic operation of distributed multifunctional single-phase grid-tie inverters in a microgrid," *IEEE Trans. Ind. Electron.*, vol. 65, no. 10, pp. 8018–8029, Oct. 2018.

[14] S. Y. M. Mousavi, A. Jalilian, M. Savaghebi, and J. M. Guerrero, "Coordinated control of multifunctional inverters for voltage support and harmonic compensation in a grid-connected microgrid," *Electr. Power Syst. Res.*, vol. 155, pp. 254–264, Feb. 2018.

[15] Z. Zeng, R. Zhao, and H. Yang, "Coordinated control of multi-functional grid-tied inverters using conductance and susceptance limitation," *IET Power Electron.*, vol. 7, no. 7, pp. 1821–1831, Jul. 2014.

[16] R. Chilipi, N. Alsayari, and A. El Aroudi, "Coordinated control of parallel operated renewable-energy-based DG systems," *IET Renew. Power Gener.*, vol. 12, no. 14, pp. 1623–1632, Oct. 2018.

[17] M. Yazdanian and A. Mehrizi-Sani, "Distributed control techniques in microgrids," *IEEE Trans. Smart Grid*, vol. 5, no. 6, pp. 2901–2909, Nov. 2014.

[18] Y. Wan, J. Cao, G. Chen, and W. Huang, "Distributed observer-based cyber-security control of complex dynamical networks," *IEEE Trans. Circuits Syst. I, Reg. Papers*, vol. 64, no. 11, pp. 2966–2975, Nov. 2017.

[19] Y. Lv, J. Fu, G. Wen, T. Huang, and X. Yu, "Distributed adaptive observer-based control for output consensus of heterogeneous MASs with input saturation constraint," *IEEE Trans. Circuits Syst. I, Reg. Papers*, vol. 67, no. 3, pp. 995–1007, Mar. 2020.

[20] X. Lu, R. Lu, S. Chen, and J. Lu, "Finite-time distributed tracking control for multi-agent systems with a virtual leader," *IEEE Trans. Circuits Syst. I, Reg. Papers*, vol. 60, no. 2, pp. 352–362, Feb. 2013.

[21] X.-M. Zhang *et al.*, "Networked control systems: A survey of trends and techniques," *IEEE/CAA J. Automatica Sinica*, vol. 7, no. 1, pp. 1–17, Jan. 2020.

[22] A. Bidram, A. Davoudi, F. L. Lewis, and J. M. Guerrero, "Distributed cooperative secondary control of microgrids using feedback linearization," *IEEE Trans. Power Syst.*, vol. 28, no. 3, pp. 3462–3470, Aug. 2013.

[23] N. M. Dehkordi, H. R. Baghaee, N. Sadati, and J. M. Guerrero, "Distributed noise-resilient secondary voltage and frequency control for islanded microgrids," *IEEE Trans. Smart Grid*, vol. 10, no. 4, pp. 3780–3790, Jul. 2019.

[24] N. Mahdian, S. S. Moghaddam, A. Khorsandi, H. R. Baghaee, N. Sadati, and J. M. Guerrero, "Voltage and frequency consensusability of autonomous microgrids over fading channels," *IEEE Trans. Energy Convers.*, early access, Jun. 26, 2020, doi: 10.1109/TEC.2020.3005269.

[25] S. Weng, D. Yue, C. Dou, J. Shi, and C. Huang, "Distributed event-triggered cooperative control for frequency and voltage stability and power sharing in isolated inverter-based microgrid," *IEEE Trans. Cybern.*, vol. 49, no. 4, pp. 1427–1439, Apr. 2019.

[26] L. Ding, Q.-L. Han, and X.-M. Zhang, "Distributed secondary control for active power sharing and frequency regulation in islanded microgrids using an event-triggered communication mechanism," *IEEE Trans. Ind. Informat.*, vol. 15, no. 7, pp. 3910–3922, Jul. 2019.

[27] X. Lu, X. Yu, J. Lai, J. M. Guerrero, and H. Zhou, "Distributed secondary voltage and frequency control for islanded microgrids with uncertain communication links," *IEEE Trans. Ind. Informat.*, vol. 13, no. 2, pp. 448–460, Apr. 2017.

[28] R. Olfati-Saber, J. A. Fax, and R. M. Murray, "Consensus and cooperation in networked multi-agent systems," *Proc. IEEE*, vol. 95, no. 1, pp. 215–233, Jan. 2007.

[29] Y. Cao, W. Ren, and Y. Li, "Distributed discrete-time coordinated tracking with a time-varying reference state and limited communication," *Automatica*, vol. 45, no. 5, pp. 1299–1305, May 2009.

[30] *IEEE Standard Definitions for the Measurement of Electric Power Quantities Under Sinusoidal, Nonsinusoidal, Balanced, or Unbalanced Conditions*, IEEE Standard 1459-2010, Mar. 2010, pp. 1–50.

[31] D. Yue, E. Tian, and Q.-L. Han, "A delay system method for designing event-triggered controllers of networked control systems," *IEEE Trans. Autom. Control*, vol. 58, no. 2, pp. 475–481, Feb. 2013.

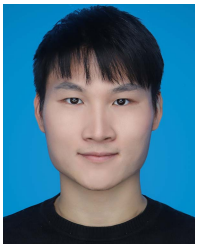

Jianbo Chen (Graduate Student Member, IEEE) received the B.S. degree from the School of Electrical Engineering and Automation, Nanjing University of Posts and Telecommunications, Nanjing, China, in 2015, where he is currently pursuing the Ph.D. degree.

His current research interests include distributed control, event-triggered control, parallel control of multiple inverters, and power quality improvement of the microgrid.

Dong Yue (Fellow, IEEE) received the Ph.D. degree from the South China University of Technology, Guangzhou, China, in 1995.

He is currently a Professor and the Dean of the Institute of Advanced Technology and the College of Automation and AI, Nanjing University of Posts and Telecommunications. He has published more than 250 articles in international journals and two books. He holds more than 50 patents. His research interests include analysis and synthesis of networked control systems, multi-agent systems, optimal control of power systems, and the Internet of Things. He has served as an Associate Editor for *IEEE Industrial Electronics Magazine*, IEEE TRANSACTIONS ON INDUSTRIAL INFORMATICS, IEEE TRANSACTIONS ON SYSTEMS, MAN AND CYBERNETICS: SYSTEMS, IEEE TRANSACTIONS ON NEURAL NETWORKS AND LEARNING SYSTEMS, *Journal of the Franklin Institute*, and *International Journal of Systems Sciences*, and the Guest Editor for Special Issue on *New Trends in Energy Internet: Artificial Intelligence-based Control, Network Security and Management* and IEEE TRANSACTIONS ON SYSTEMS, MAN, AND CYBERNETICS: SYSTEMS.

Chunxia Dou (Member, IEEE) received the B.S. and M.S. degrees in automation from the Northeast Heavy Machinery Institute, Qiqihaer, China, in 1989 and 1994, respectively, and the Ph.D. degree in measurement technology and instrumentation from the Institute of Electrical Engineering, Yanshan University, Qinhuangdao, China, in 2005.

In 2010, she joined the Department of Engineering, Peking University, Beijing, China, where she was a Post-Doctoral Fellow for two years. Since 2005, she has been a Professor with the Institute of Electrical Engineering, Yanshan University, and a Professor with the Institute of Advanced Technology, Nanjing University of Posts and Telecommunications, Nanjing, China. Her current research interests include multiagent-based control, event-triggered hybrid control, distributed coordinated control, and multimode switching control and their applications in power systems, microgrids, and smart grids.

Ye Li received the B.S. degree in automation and the M.S. degree in control engineering from the Dalian University of Technology, Dalian, China, in 2012 and 2014, respectively.

She is currently an Engineer with Shanghai KeLiang Technology and Engineering Company Ltd., mainly engaged in simulation modeling of power systems and power electronics.

Gerhard P. Hancke (Life Fellow, IEEE) received the B.Sc., B.Eng., and M.Eng. degrees in electronic engineering from the University of Stellenbosch, South Africa, in 1970 and 1973, respectively, and the D.Eng. degree from the University of Pretoria, South Africa, in 1983.

He is currently a Professor with the Nanjing University of Posts and Telecommunications, China, and the University of Pretoria. He is recognized internationally as a pioneer and a leading scholar in the Industrial Wireless Sensor Networks research. He initiated and co-edited the first Special Section on *Industrial Wireless Sensor Networks* in the IEEE TRANSACTIONS ON INDUSTRIAL ELECTRONICS, in 2009 and the IEEE TRANSACTIONS ON INDUSTRIAL INFORMATICS, in 2013. He co-edited a textbook, *Industrial Wireless Sensor Networks: Applications, Protocols and Standards* (2013), the first on the topic. He has been serving as an Associate Editor and Guest Editor for the IEEE TRANSACTIONS ON INDUSTRIAL INFORMATICS, IEEE ACCESS, and the IEEE TRANSACTIONS ON INDUSTRIAL ELECTRONICS. He is currently the Co-Editor-in-Chief of the IEEE TRANSACTIONS ON INDUSTRIAL INFORMATICS and a Senior Editor of IEEE ACCESS.

Shengxuan Weng received the B.S. degree from the School of Mathematics and Statistics, Huazhong University of Science and Technology, Wuhan, China, in 2009, and the Ph.D. degree from the School of Automation, Huazhong University of Science and Technology, in 2014.

Since 2014, he has been with the Institute of Advanced Technology, Nanjing University of Posts and Telecommunications, Nanjing, China. His current research interests include distributed control, multiagent systems, and control approach in microgrid and smart grid.

Josep M. Guerrero (Fellow, IEEE) received the B.S. degree in telecommunications engineering, the M.S. degree in electronics engineering, and the Ph.D. degree in power electronics from the Technical University of Catalonia, Barcelona, in 1997, 2000, and 2003, respectively.

Since 2011, he has been a Full Professor with the Department of Energy Technology, Aalborg University, Denmark, where he is responsible for the Microgrid Research Program. Since 2014, he has been a Chair Professor with Shandong University and a Distinguished Guest Professor with Hunan University. Since 2016, he has been a Visiting Professor Fellow with Aston University, U.K., and a Guest Professor with the Nanjing University of Posts and Telecommunications. Since 2019, he became a Villum Investigator by The Villum Fonden, which supports the Center for Research on Microgrids (CROM), Aalborg University. He is the Founder and the Director of the CROM (www.crom.et.aau.dk). His research interests include oriented to different microgrid aspects, including power electronics, distributed energy-storage systems, hierarchical and cooperative control, energy management systems, smart metering, and the Internet of Things for AC/DC microgrid clusters and islandeminigrids. Specially focused on microgrid technologies applied to offshore wind, maritime microgrids for electrical ships, vessels, ferries and seaports, and space microgrids applied to nanosatellites and spacecrafts. He has published more than 600 journal articles in the fields of microgrids and renewable energy systems, which are cited more than 50,000 times. In 2015, he was elevated as a IEEE Fellow for his contributions on distributed power systems and microgrids. He received the Best Paper Award from the IEEE TRANSACTIONS ON ENERGY CONVERSION from 2014 to 2015 and the *Journal of Power Electronics* in 2016 and the Best Paper Prize from IEEE-PES in 2015. He is an Associate Editor for a number of IEEE TRANSACTIONS. During seven consecutive years, from 2014 to 2020, he was awarded by Clarivate Analytics (former Thomson Reuters) as Highly Cited Researcher with 50 highly cited articles.

Xiaohua Ding received the master's degree from the Zhejiang University of Power System Automation in 1999.

He is working with Nari Technology Development Company Ltd. His main research interests include distribution automation, active distribution networks, and demand side management.